THE JOURNAL OF PHYSICAL CHEMISTRY C

Article

pubs.acs.org/JPCC

Tailoring the Growth of Graphene on Ru(0001) via Engineering of the Substrate Surface

Li Jin, Qiang Fu,* Hui Zhang, Rentao Mu, Yanhong Zhang, Dali Tan, and Xinhe Bao

State Key Laboratory of Catalysis, Dalian Institute of Chemical Physics, The Chinese Academy of Sciences, Dalian 116023, P.R. China

Supporting Information

ABSTRACT: In situ low-energy electron microscopy (LEEM) studies in the epitaxial growth of graphene on Ru(0001) show that the graphene growth can be tailored via surface treatments of the substrate. Downhill growth of graphene was observed over the clean Ru(0001) surface with well-defined steps, forming sector-shaped graphene sheets. When the substrate surface was treated by Ar^+ sputtering to produce subsurface Ar gas bubbles, round-shape graphene sheets were obtained by growing in both uphill and downhill directions. Correspondingly, anisotropic intercalation of oxygen occurs at the graphene/normal Ru(0001) interface, whereas isotropic intercalation of oxygen occurs at the graphene/Ar-sputtered Ru(0001) interface. The subsurface gas bubbles affect C−Ru interaction, which is attributed to the observed different behaviors of the graphene growth and oxygen intercalation.

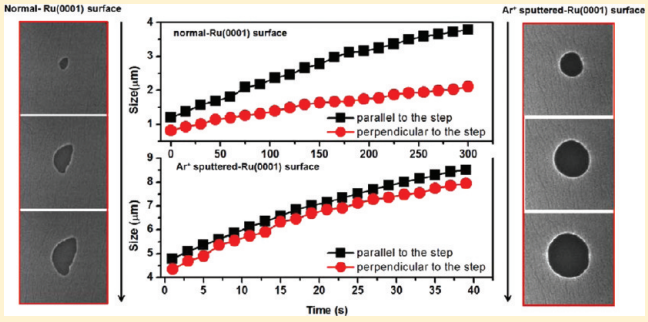

INTRODUCTION

Graphene has attracted extensive attention due to its fascinating physical and chemical properties.[1,2] Controllable growth of high-quality graphene structures is essential to the potential applications of the new material, and epitaxial growth on metals has been regarded as one of the most important routes.[3−9] Various factors such as metal substrates, carbon precursors, growth temperature, and pressure have been shown to affect the growth mechanism.[10−19]

Many experimental and theoretical results have indicated that the graphene growth depends strongly on the interaction between graphene and metals. Generally, two classes of graphene−metal interactions can be identified: physisorption and chemisorption.[20] For example, graphene is strongly chemisorbed on Ru(0001) via significant hybridization of C p_z states and Ru d states.[5,21,22] In the initial stage of the graphene growth on Ru(0001), identical-size 7-C6 and 3-C6 graphene nanoclusters form on the Ru(0001) terraces, which is thought to be mediated by the substrate-induced clustering effect.[23] At higher temperatures, the lower edges of the substrate steps are found to be the preferential nucleation sites for graphene sheets.[11,24,25] Downhill growth of graphene was almost exclusively observed, producing continuous sector-shaped carpets across descending substrate steps.[5,13,15,26] Graphene on Pt(111) is a typical system with weak interfacial bonding. In the nucleation stage, the surface carbon nanostructures are inhomogeneous.[23,27] Following the nucleation, each graphene domain expands by attachment of carbon to its edge, which produces a single-crystalline graphene sheet. In contrast to the unidirectional growth on Ru(0001), graphene expands across the Pt(111) steps in the uphill and downhill directions.[9] The climbing up growth of graphene sheets over substrate steps has been observed on Cu(111) and Ir(111) surfaces, which also interact weakly with graphene.[7,8,19]

The previous results indicate that the interaction of carbon with a metal substrate controls the epitaxial growth of graphene. The strong interaction of carbon atoms with metal surfaces, in particular, the step sites, tends to pin one edge of the graphene domain and suppress the uphill growth. In contrast, the weak carbon−metal interaction leads to the trivial role of the surface defects in the graphene growth, and therefore, anisotropic growth of graphene occurs. It is known that solid surfaces can be effectively engineered via surface treatments, which affect the interaction of adsorbates with the substrates.[28] Hence, the surface engineering of the metal substrates can be made to tune the carbon−metal interaction and the graphene growth atop.

In the present work, a simple way to modify the Ru(0001) surfaces was attempted by Ar^+ sputtering followed by annealing at moderately high temperatures (below 1000 °C). Introduction of subsurface Ar gas bubbles at the Ru(0001) surface changes the carbon−substrate interaction and the graphene growth. The present results demonstrate an effective route to attain the controllable growth of graphene on metals.

EXPERIMENT

In situ low-energy electron microscopy (LEEM) experiments were carried out in an Elmitec LEEM system, which contains a

Received: October 24, 2011
Revised: December 9, 2011
Published: December 30, 2011

dx.doi.org/10.1021/jp210206y | J. Phys. Chem. C 2012, 116, 2988−2993

preparation chamber, an imaging system, and a vacuum ultraviolet (VUV) laser source (λ = 177.3 nm).[29] The preparation chamber is equipped with an Ar^+ sputtering gun and two effusion cells. The imaging system has a hemispheric analyzer, an aberration corrector, a field emission electron source, and other electron lenses.

The Ru(0001) surface was prepared by cycled Ar^+ sputtering (2.0 KeV, 7×10^{-6} Torr Ar, 10 min), heating in O_2 (530 °C, 5×10^{-7} Torr O_2), and annealing in ultrahigh vacuum (UHV) at high temperatures (e.g., 1200 °C).[11,26] The clean Ru(0001) surface was then deliberately doped with carbon via exposure to 10 Langmuir (L) ethylene (C_2H_4) at 900 °C for the graphene growth through the surface segregation process. Alternatively, the graphene growth can be carried out on the clean Ru(0001) surface by chemical vapor deposition (CVD). The growth processes were monitored by in situ LEEM. High-purity gases, such as C_2H_4 and O_2, were introduced onto the surface by backfilling the chamber with the partial pressure up to 1×10^{-6} Torr.

Scanning tunneling microscopy (STM) measurements were conducted on an Omicron multiprobe UHV system.[11,23] The Ru(0001) surface was cleaned in a preparation chamber and investigated in an imaging chamber, in which a variable-temperature STM was installed. STM was conducted in the constant current mode at room temperature using a homemade tungsten (W) tip.

In both UHV systems, the samples can be heated to 1700 °C via electron bombardment at the backside of the sample. The sample temperature was measured by a W–Re thermocouple welded at the sample stages or by an infrared thermometer (Land Cyclops 100).

RESULTS AND DISCUSSIONS

To prepare the well-defined Ru(0001) surface, cycled Ar^+ sputtering, heating in O_2, and annealing in UHV above 1200 °C have to be performed. As shown in Figure 1a, the surface

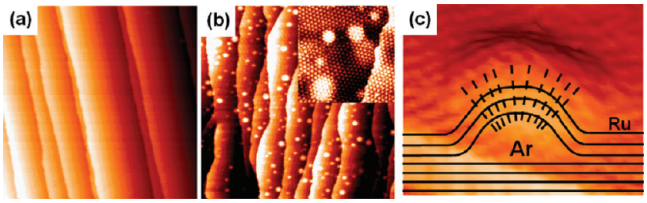

Figure 1. STM images from the normal-Ru(0001) surface (a) (V = 0.2 V, I = 0.6 nA, 200 nm × 200 nm) and the sputtered-Ru(0001) surface (b) (V = 0.2 V, I = 0.5 nA, 500 nm × 500 nm). The inset (V = 0.1 V, I = 2.2 nA, 100 nm × 100 nm) in (b) shows the monolayer graphene on the sputtered-Ru(0001) surface. (c) The scheme of an Ar bubble at the Ru(0001) subsurface.

treated by this process is atomically flat and has straight steps, which is called the normal-Ru(0001) surface in this work. When the surface was finally sputtered for 1 h and annealed in UHV below 1000 °C (denoted as the sputtered-Ru(0001) surface), a high density of surface protrusions (about 8×10^{14} m^{-2}) can be observed, although the surface was still flat and uniformly stepped (Figure 1b). The effect of Ar^+ sputtering on metal surface structures has been carefully studied by Menzel et al. and Varga et al.[30−32] It has been shown that stable subsurface cavities filled with hundreds of Ar atoms can be produced by the Ar^+ ion bombardment or implantation.[30] Annealing at moderately high temperatures, e.g., 1200 K, heals the sputter damage at the surface, but the Ar bubbles are still embedded in the subsurface layers.[31] Only by annealing at temperatures above 1200 °C may it be possible to remove the surface protrusions through dissolution of Ar into the bulk or desorption of Ar from the surface. The protrusions observed on the sputtered-Ru(0001) surface have lateral size ranging from several nanometers to tens of nanometers and a height of a few angstroms (Figure 1b). Local strains are produced at the Ru(0001) outermost layers by covering the bubbles. The lattice is stretched above the bubbles while compressed at the edges of the protrusions (Figure 1c).[32]

The growth of graphene on the above-mentioned surfaces was attempted by the surface segregation process. On the normal-Ru(0001) surface doped with carbon, the sample was first annealed at temperatures above 1200 °C and then cooled below 800 °C. The graphene growth was monitored by LEEM. The energy of the incident electrons was set around 3.5 eV to have a sharp contrast between the carbon adatoms and the newly formed graphene domain.[13] As shown in Figures 2a–c, each graphene domain nucleates at the substrate steps (marked by red dashed line) and expands quickly in three directions (the video can be found in Figure S1 of the Supporting Information). Finally, a typical sector-shaped graphene sheet forms with one edge pinned by the substrate step. The size of the graphene domain in the dimensions parallel and perpendicular to the steps is almost 2:1 (the upper panel of Figure 2g), similar to our previous findings.[26] Thus, the graphene growth on the normal-Ru(0001) surface follows the typical downhill growth mode.[5,13,15,26]

Figures 2d–f show the growth of graphene on a sputtered-Ru(0001) surface. Starting from the nucleation site at a step, the graphene domain expands equally in every direction (the video can be found in Figure S2, Supporting Information). The isotropic growth of graphene produces round-shaped sheets in micrometers. The size of the graphene domain in the dimensions which are parallel and perpendicular to the step is displayed in the lower panel of Figure 2g. The ratio of these two dimensions is kept at 1:1. The round-shaped graphene islands can be dissolved in the near-surface region of Ru(0001) by annealing the surface above 1000 °C.[12,33] Subsequently, the isotropic growth and dissolution of graphene islands can be cycled when the surface temperature changes between 700 and 1000 °C. However, once the surface was flashed at temperatures higher than 1200 °C, graphene grows on the surface in an anisotropic way.

CVD was also applied to grow graphene on the undoped normal-Ru(0001) surface and sputtered-Ru(0001) surface. On these two surfaces, ethylene was leaked to a pressure of 1×10^{-8} Torr, and the substrate temperature was kept at 780 °C. In situ LEEM imaging shows that sector-shaped graphene islands were obtained on the normal-Ru(0001) surface, whereas the round-shaped graphene sheets formed on the sputtered-Ru(0001) surface. The corresponding videos are displayed in Figures S3 and S4 (Supporting Information). The results are similar to those obtained with the surface segregation process.

Spatially resolved low-energy electron diffraction (LEED) measurements were carried out to study the surface structure of the sector-shaped and round-shaped graphene sheets. The LEED patterns from the two graphene surfaces have the same symmetry and periodicity, which indicate a (12 × 12)-C on (11 × 11)-Ru moiré superstructure of monolayer graphene on Ru(0001) (insets in Figures 3a and 3b).[6,15,34,35] The diffraction spots from the graphene/normal-Ru(0001) surface are quite

dx.doi.org/10.1021/jp210206y | J. Phys. Chem. C 2012, 116, 2988–2993

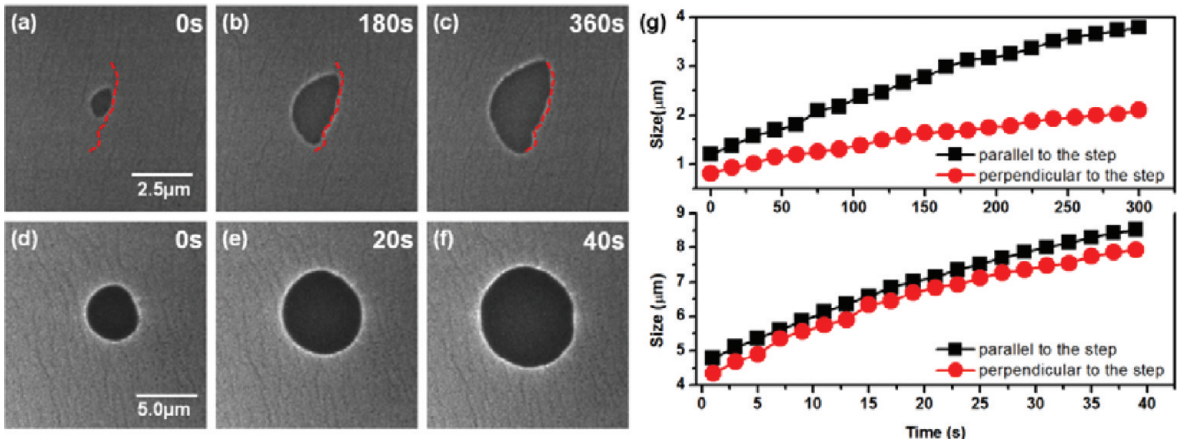

Figure 2. Series of LEEM images recording the graphene growth on the normal-Ru(0001) surface (a–c) and on the sputtered-Ru(0001) surface (d–f) through the surface segregation with the surface temperature at 690 and 790 °C, respectively. The red dashed lines in (a–c) mark the step. The videos can be found in Figures S1 and S2, Supporting Information. The start voltage for the images of a–c is 3.7 V and 3.2 V for the images of d–f. (g) Plots of the dimensions of the graphene sheets parallel (squares) and perpendicular (circles) to the steps versus the segregation time on the normal-Ru(0001) surface (upper panel) and on the sputtered-Ru(0001) surface (lower panel).

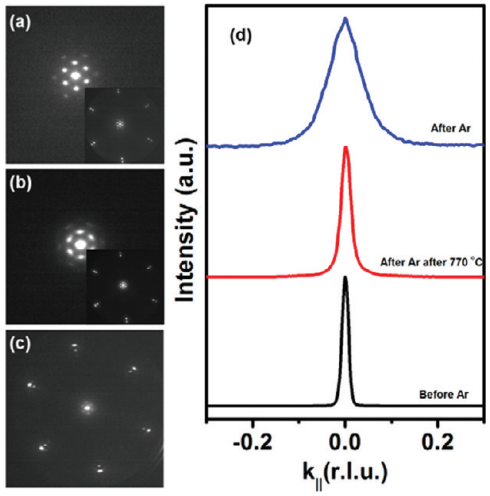

Figure 3. Spatially resolved LEED patterns recorded from (a) the graphene/normal-Ru(0001) surface (50 eV) and (b) the graphene/sputtered-Ru(0001) surface (50 eV) prepared by the surface segregation method at 770 °C. The insets show the LEED patterns including the specular beam and the first-order diffraction spots. (c) A LEED pattern from the O-intercalated graphene/Ru(0001) surface (60 eV). (d) The intensity profiles of the central diffraction spots from the normal Ru(0001) surface, the Ar-sputtered Ru(0001) surface, and the Ar-sputtered Ru(0001) annealed at 770 °C in UHV. The width of the primary spot is with respect to the Ru lattice. The probe area for the LEED measurements is about 5 μm.

sharp (Figure 3a), whereas those from the graphene/sputtered-Ru(0001) surface become diffuse and broadened (Figure 3b). For one aspect, we observed the azimuthal broadening of the diffraction spots, which can be ascribed to the in-plane disorder structure on the sputtered surface. At the same time, the radical broadening of the spots is also present on the sputtered surface. Since the monolayer graphene duplicates the surface morphology of the substrate, the similar change in the LEED pattern should occur on the bare substrate. LEED patterns have been acquired from the normal-Ru(0001) surface, the sputtered Ru(0001) surface, and the sputtered Ru(0001) surface annealed at 770 °C. The intensity profiles of the (00) spots were shown in Figure 3d. Obviously, the sputtering produces surface defects, which results in strong broadening of the spot. After annealing at 770 °C, the spot is still much broader than that from the normal-surface. Although the surface defects are mostly healed, the subsurface Ar bubbles still remain.[31,32] Thus, the broadening should be ascribed to the surface roughness induced by the surface Ar bubbles. Locatelli et al. have applied microprobe LEED to measure the surface corrugation on SiO_2-supported and suspended exfoliated graphene structures. They suggested that the broadening of the diffraction spots can be attributed to the increase in corrugations of the graphene structures.[36] Knox et al. have found that the width of the LEED spots increased with the decreasing graphene layer number, which reached a maximum for monolayer graphene on the SiO_2 substrate. The thin graphene sheets conform to the rough SiO_2 surface, while thick sheets are too stiff to follow the contour of the substrate.[37] The surface roughening may imply a mosaic tilting of small flat areas of the surface, such that the diffracted beams from each titled surface area are projected to different angular directions.[38−40] As a result, the observed broadened LEED spots indicate the rough surface of the sputtered substrate due to the subsurface Ar bubbles.

The protrusions of the subsurface Ar bubbles can be further imaged using mirror electron microscopy (MEM), in which the electron beam is backscattered by the retarding field before striking the sample surfaces and is therefore more sensitive to the topographical features.[41,42] In the MEM mode, many black dots are visible at the bare sputtered-Ru(0001) and graphene/sputtered-Ru(0001) surfaces under an overfocus condition, while they are white dots in an under-focus mode (Figure 4 and Figure S5, Supporting Information). Since MEM shows the profile of the surface-retarding field, the size of a surface feature in the MEM image is much larger than the real one. For example, Shimakura et al. reported that the size of surface protrusions in a MEM image is actually 8 times bigger than that in an atomic force microscopy (AFM) image.[43] Considering this difference, it is reasonable to conclude that the dots in the MEM images are the same with the surface protrusions observed by STM at the sputtered-Ru(0001) surface (Figure 1b) and the graphene-covered surface (inset of Figure 1b). It should be noted that similar structures cannot be observed at the normal-Ru(0001) surface under the same imaging conditions.

dx.doi.org/10.1021/jp210206y | J. Phys. Chem. C 2012, 116, 2988−2993

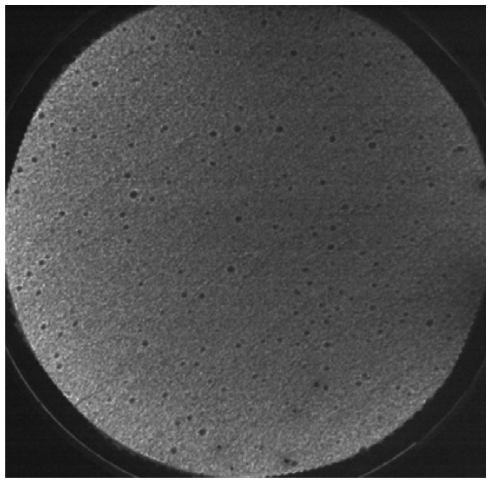

Figure 4. MEM image obtained from a graphene/sputtered-Ru(0001) surface. The field of view (FoV) is 10 μm, and the start voltage (STV) is −0.1 V.

The above results clearly show that the subsurface Ar bubbles largely affect the growth of graphene on Ru(0001). When one edge of a graphene domain encounters the lower edge of a surface step at the normal-Ru(0001) surface, there would be a maximum overlap of the graphene edge states with the Ru step. Once the edge becomes saturated, carbon clusters would preferentially attach to the other part of the domain edge. Therefore, the surface steps play a critical role in the graphene growth, resulting in the downhill growth. For the sputtered-Ru(0001) surface, the C−Ru interaction on the terraces is modified by the subsurface Ar bubbles. As discussed above, the Ru(0001) outermost layers above the bubbles are bended upward, and then the Ru(0001) surface lattice is stretched. Mavrikakis et al. have shown that surface reactivity of Ru(0001) increases as a result of the lattice expansion, along with a concurrent upshift of the metal d states.[44,45] Therefore, the building up of the stretching strain at the Ru(0001) surface layers above the bubbles may strengthen the C−Ru interaction therein. Accordingly, we infer that carbon may interact similarly with terraces and steps at the sputtered-Ru(0001) surface. In such a case, carbon clusters attach all edges of each graphene domain equally, resulting in the observed isotropic expansion of the graphene sheets.

The enhanced C−Ru interaction on the terraces of the sputtered-Ru(0001) surface can also be proved by the dissolution of the graphene islands at high temperatures. Upon annealing at 850 °C, the round-shaped graphene islands start to get dissolved from inside of the islands but not from the island edges, in contrast with the case of the sector-shaped graphene islands (Figure 5 and Figure S6, Supporting Information). Obviously, the preferential dissolution from the inner parts of the graphene sheets is facilitated by the strong graphene−substrate interaction at the Ru(0001) terraces.

The treatment of the Ru(0001) surface via the Ar^+ sputtering can be used to tune the intercalation reaction at the graphene/Ru(0001) interfaces, which is also related to the graphene−metal interaction. It has been shown that molecules and elements can be intercalated underneath graphene layers grown on metals.[11,29,35,46−49] We have proposed an intercalation mechanism at the graphene/metal interfaces, in which the intercalating atoms need to break the bonding between

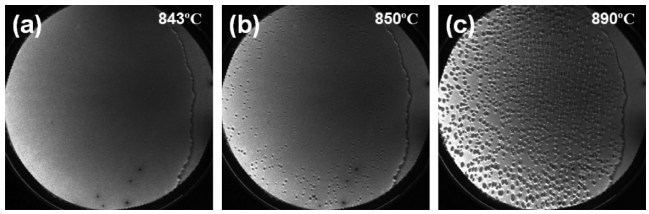

Figure 5. Series of MEM images of a graphene/sputtered-Ru(0001) surface annealed in UHV at various temperatures: (a) 843 °C; (b) 850 °C; (c) 890 °C. The FoV is 50 μm, and the STV is −0.1 V. The video can be found in Figure S6 (Supporting Information).

graphene edge atoms and the substrate surface atoms and to diffuse under the graphene surface.[29]

Both the graphene/normal-Ru(0001) surface and the graphene/sputtered-Ru(0001) surface were exposed to 3×10^{-7} Torr O_2 at 330 °C. The occurrence of oxygen intercalation leads to the changes in image contrast which can be monitored by LEEM sensitively. Moreover, spatially resolved LEED patterns acquired from the O-intercalated graphene region show that the satellite spots of the moiré superstructure are strongly suppressed (Figure 3c).[29,50−54] This result confirms our previous STM observation that O-intercalation at the graphene/Ru(0001) interface decouples the monolayer graphene structure from the substrate and makes the graphene layer free-standing.[11]

On the graphene/normal-Ru(0001) surface, O intercalation took place only from the sector edge of the sector-shaped graphene island, and the intercalation at the edge that pinned to the substrate step was inhibited (Figure 6a−c, and the video can be found in Figure S7, Supporting Information). The ratio of the dimensions of the unintercalated graphene region parallel and perpendicular to the step is kept at 2:1 (upper panel of Figure 6g). This is consistent with the results reported by McCarty and co-workers.[46] On the sputtered-Ru(0001) surface, O intercalation started to occur at the whole edge of the graphene sheet and proceeded toward the center of the island at the same speed (Figure 6d−f, and the video can be found in Figure S8, Supporting Information). The dimensions of the unintercalated graphene region parallel and perpendicular to the step were measured, which shows that this region shrinks inward homogeneously (lower panel of Figure 6g). The in situ LEEM data confirm anisotropic intercalation of oxygen on the normal-Ru(0001) surface but isotropic intercalation on the sputtered-Ru(0001) surface. The stronger bonding of the edge carbon atoms with the lower edges of the substrate steps than that of the edge atoms with the terraces results in the preferential breaking of C−Ru bonding at the sector edge via atomic oxygen. On the other hand, the enhanced C−Ru interaction between graphene and Ru(0001) terraces due to the subsurface Ar bubbles enables the occurrence of the intercalation from the whole edge of the graphene sheet, which is consistent with the growth procedure.

■ CONCLUSION

Anisotropic and isotropic epitaxial growth of graphene sheets was observed on the well-defined Ru(0001) surface and the Ru(0001) surface treated by Ar^+ sputtering, respectively. It is found that the Ar^+ sputtering followed by annealing at moderately high temperature (between 700 and 1000 °C) produces subsurface Ar bubbles at the flat Ru(0001) surface. The strain at the topmost Ru(0001) layers above the bubbles

dx.doi.org/10.1021/jp210206y | J. Phys. Chem. C 2012, 116, 2988−2993

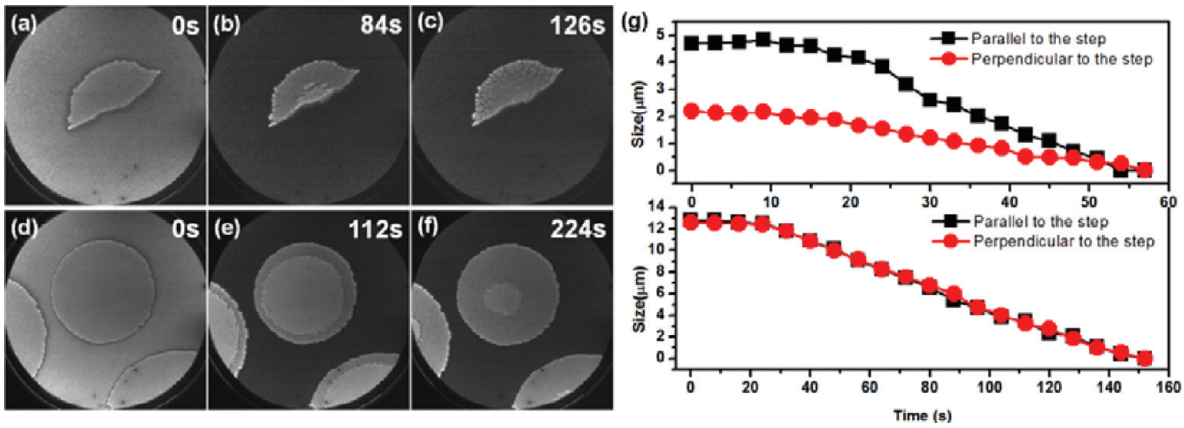

Figure 6. Series of LEEM images showing the O intercalation at the graphene/normal-Ru(0001) interface (a–c, FoV = 10 μm, STV = 3.3 V) and at the graphene/sputtered-Ru(0001) interface (d–f, FoV = 25 μm, STV = 3.3 V) at the indicated intercalating time. The videos can be found in Figures S7 and S8 (Supporting Information). (g) Plots of the dimensions of the unintercalated graphene regions parallel (squares) and perpendicular (circles) to the step versus the intercalating time on the graphene/normal-Ru(0001) interface (upper panel) and on the graphene/sputtered-Ru(0001) interface (lower panel).

strengthens the C–Ru interaction at the Ru(0001) terraces, reducing the effect of the surface steps on the graphene growth. At the same time, the presence of subsurface Ar bubbles also results in isotropic intercalation of oxygen under the graphene sheets on the sputtered Ru(0001) in contrast to the anisotropic intercalation between graphene and the well-defined surface. The present results demonstrate that the epitaxial growth of graphene can be simply controlled via surface engineering of the substrates. This methodology provides a chance to tailor graphene growth on solid substrates.

■ ASSOCIATED CONTENT

Supporting Information

Figures S1–S8. This material is available free of charge via the Internet at http://pubs.acs.org.

■ AUTHOR INFORMATION

Corresponding Author

*Tel.: +86-411-84379253. Fax: +86-411-84694447. E-mail: qfu@dicp.ac.cn.

■ ACKNOWLEDGMENTS

This work was financially supported by the National Natural Science Foundation of China (No. 20873143, No. 21073183, and No. 21033009), Ministry of Science and Technology of China (No. 2011CB932700), and Chinese Academy of Sciences ("Bairen" program). We acknowledge the fruitful discussions with Prof. Weixue Li.

■ REFERENCES

(1) Novoselov, K. S.; Geim, A. K.; Morozov, S. V.; Jiang, D.; Katsnelson, M. I.; Grigorieva, I. V.; Dubonos, S. V.; Firsov, A. A. Two-dimensional gas of massless Dirac fermions in graphene. *Nature* **2005**, *438*, 197–200.

(2) Geim, A. K.; Novoselov, K. S. The rise of graphene. *Nat. Mater.* **2007**, *6*, 183–191.

(3) Geim, A. K. Graphene: Status and Prospects. *Science* **2009**, *324*, 1530–1534.

(4) Wintterlin, J.; Bocquet, M. L. Graphene on metal surfaces. *Surf. Sci.* **2009**, *603*, 1841–1852.

(5) Sutter, P. W.; Flege, J. I.; Sutter, E. A. Epitaxial graphene on ruthenium. *Nat. Mater.* **2008**, *7*, 406–411.

(6) Pan, Y.; Zhang, H. G.; Shi, D. X.; Sun, J. T.; Du, S. X.; Liu, F.; Gao, H. J. Highly Ordered, Millimeter-Scale, Continuous, Single-Crystalline Graphene Monolayer Formed on Ru (0001). *Adv. Mater.* **2009**, *21*, 2777–2780.

(7) Coraux, J.; N'Diaye, A. T.; Engler, M.; Busse, C.; Wall, D.; Buckanie, N.; Heringdorf, F. J. M. Z.; van Gastei, R.; Poelsema, B.; Michely, T. Growth of graphene on Ir(111). *New J. Phys.* **2009**, *11*, 023006.

(8) Gao, L.; Guest, J. R.; Guisinger, N. P. Epitaxial Graphene on Cu(111). *Nano Lett.* **2010**, *10*, 3512–3516.

(9) Sutter, P. W.; Sadowski, J. T.; Sutter, E. A. Graphene on Pt(111): Growth and substrate interaction. *Phys. Rev. B: Condens. Matter Mater. Phys.* **2009**, *80*, 245411.

(10) Li, X. S.; Cai, W. W.; An, J. H.; Kim, S.; Nah, J.; Yang, D. X.; Piner, R.; Velamakanni, A.; Jung, I.; Tutuc, E. Large-Area Synthesis of High-Quality and Uniform Graphene Films on Copper Foils. *Science* **2009**, *324*, 1312–1314.

(11) Zhang, H.; Fu, Q.; Cui, Y.; Tan, D. L.; Bao, X. H. Growth Mechanism of Graphene on Ru(0001) and O_2 Adsorption on the Graphene/Ru(0001) Surface. *J. Phys. Chem. C.* **2009**, *113*, 8296–8301.

(12) Cui, Y.; Fu, Q.; Tan, D. L.; Bao, X. H. Temperature Dependence of the Formation of Graphene and Subsurface Carbon on Ru(0001) and Its Effect on Surface Reactivity. *ChemPhysChem* **2010**, *11*, 995–998.

(13) Loginova, E.; Bartelt, N. C.; Feibelman, P. J.; McCarty, K. F. Evidence for graphene growth by C cluster attachment. *New J. Phys.* **2008**, *10*, 093026.

(14) Wang, B.; Ma, X. F.; Caffio, M.; Schaub, R.; Li, W. X. Size-Selective Carbon Nanoclusters as Precursors to the Growth of Epitaxial Graphene. *Nano Lett.* **2011**, *11*, 424–430.

(15) McCarty, K. F.; Feibelman, P. J.; Loginova, E.; Bartelt, N. C. Kinetics and thermodynamics of carbon segregation and graphene growth on Ru(0001). *Carbon* **2009**, *47*, 1806–1813.

(16) Rim, K. T.; Siaj, M.; Xiao, S. X.; Myers, M.; Carpentier, V. D.; Liu, L.; Su, C. C.; Steigerwald, M. L.; Hybertsen, M. S.; McBreen, P. H. Forming aromatic hemispheres on transition-metal surfaces. *Angew. Chem., Int. Ed.* **2007**, *46*, 7891–7895.

(17) Li, Z. C.; Wu, P.; Wang, C. X.; Fan, X. D.; Zhang, W. H.; Zhai, X. F.; Zeng, C. G.; Li, Z. Y.; Yang, J. L.; Hou, J. G. Low-Temperature Growth of Graphene by Chemical Vapor Deposition Using Solid and Liquid Carbon Sources. *ACS Nano* **2011**, *5*, 3385–3390.

(18) Sun, Z. Z.; Yan, Z.; Yao, J.; Beitler, E.; Zhu, Y.; Tour, J. M. Growth of graphene from solid carbon sources. *Nature* **2010**, *468*, 549–552.

(19) Loginova, E.; Bartelt, N. C.; Feibelman, P. J.; McCarty, K. F. Factors influencing graphene growth on metal surfaces. *New J. Phys.* **2009**, *11*, 063046.
(20) Khomyakov, P. A.; Giovannetti, G.; Rusu, P. C.; Brocks, G.; van den Brink, J.; Kelly, P. J. First-principles study of the interaction and charge transfer between graphene and metals. *Phys. Rev. B: Condens. Matter Mater. Phys.* **2009**, *79*, 195425.
(21) Preobrajenski, A. B.; Ng, M. L.; Vinogradov, A. S.; Martensson, N. Controlling graphene corrugation on lattice-mismatched substrates. *Phys. Rev. B: Condens. Matter Mater. Phys.* **2008**, *78*, 073401.
(22) Gao, M.; Pan, Y.; Zhang, C. D.; Hu, H.; Yang, R.; Lu, H. L.; Cai, J. M.; Du, S. X.; Liu, F.; Gao, H. J. Tunable interfacial properties of epitaxial graphene on metal substrates. *Appl. Phys. Lett.* **2010**, *96*, 053109.
(23) Cui, Y.; Fu, Q.; Zhang, H.; Bao, X. H. Formation of identical-size graphene nanoclusters on Ru(0001). *Chem. Commun.* **2011**, *47*, 1470−1472.
(24) Marchini, S.; Gunther, S.; Wintterlin, J. Scanning tunneling microscopy of graphene on Ru(0001). *Phys. Rev. B: Condens. Matter Mater. Phys.* **2007**, *76*, 075429.
(25) Donner, K.; Jakob, P. Structural properties and site specific interactions of Pt with the graphene/Ru(0001) moire overlayer. *J. Chem. Phys.* **2009**, *131*, 164701.
(26) Cui, Y.; Fu, Q.; Zhang, H.; Tan, D. L.; Bao, X. H. Dynamic Characterization of Graphene Growth and Etching by Oxygen on Ru(0001) by Photoemission Electron Microscopy. *J. Phys. Chem. C* **2009**, *113*, 20365−20370.
(27) Levy, N.; Burke, S. A.; Meaker, K. L.; Panlasigui, M.; Zettl, A.; Guinea, F.; Neto, A. H. C.; Crommie, M. F. Strain-Induced Pseudo-Magnetic Fields Greater Than 300 T in Graphene Nanobubbles. *Science* **2010**, *329*, 544−547.
(28) Fu, Q.; Wagner, T. Interaction of nanostructured metal overlayers with oxide surfaces. *Surf. Sci. Rep.* **2007**, *62*, 431−498.
(29) Jin, L.; Fu, Q.; Mu, R. T.; Tan, D. L.; Bao, X. H. Pb intercalation underneath a graphene layer on Ru(0001) and its effect on graphene oxidation. *Phys. Chem. Chem. Phys.* **2011**, *13*, 16655−16660.
(30) Schmid, M.; Hebenstreit, W.; Varga, P.; Crampin, S. Quantum wells and electron interference phenomena in Al due to subsurface noble gas bubbles. *Phys. Rev. Lett.* **1996**, *76*, 2298−2301.
(31) Jakob, P.; Gsell, M.; Menzel, D. Interactions of adsorbates with locally strained substrate lattices. *J. Chem. Phys.* **2001**, *114*, 10075−10085.
(32) Gsell, M.; Jakob, P.; Menzel, D. Effect of substrate strain on adsorption. *Science* **1998**, *280*, 717−720.
(33) Cui, Y.; Fu, Q.; Bao, X. H. Dynamic observation of layer-by-layer growth and removal of graphene on Ru(0001). *Phys. Chem. Chem. Phys.* **2010**, *12*, 5053−5057.
(34) Martoccia, D.; Willmott, P. R.; Brugger, T.; Bjorck, M.; Gunther, S.; Schleputz, C. M.; Cervellino, A.; Pauli, S. A.; Patterson, B. D.; Marchini, S. Graphene on Ru(0001): A 25 × 25 supercell. *Phys. Rev. Lett.* **2008**, *101*, 126102.
(35) Sutter, P. W.; Sadowski, J. T.; Sutter, E. A. Chemistry under Cover: Tuning Metal-Graphene Interaction by Reactive Intercalation. *J. Am. Chem. Soc.* **2010**, *132*, 8175−8179.
(36) Locatelli, A.; Knox, K. R.; Cvetko, D.; Mentes, T. O.; Nino, M. A.; Wang, S. C.; Yilmaz, M. B.; Kim, P.; Osgood, R. M.; Morgante, A. Corrugation in Exfoliated Graphene: An Electron Microscopy and Diffraction Study. *ACS Nano* **2010**, *4*, 4879−4889.
(37) Knox, K. R.; Wang, S. C.; Morgante, A.; Cvetko, D.; Locatelli, A.; Mentes, T. O.; Nino, M. A.; Kim, P.; Osgood, R. M. Spectromicroscopy of single and multilayer graphene supported by a weakly interacting substrate. *Phys. Rev. B: Condens. Matter Mater. Phys.* **2008**, *78*, 201408.
(38) Peale, D. R.; Haight, R.; LeGoues, F. K. Strain Relaxation in Ultrathin Epitaxial-Films of Beta-$FeSi_2$ on Unstrained and Strained Si(100) Surfaces. *Thin Solid Films* **1995**, *264*, 28−39.
(39) Theilmann, F.; Matzdorf, R.; Meister, G.; Goldmann, A. Influence of surface structural disorder on linewidths in angle-resolved photoemission spectra. *Phys. Rev. B: Condens. Matter Mater. Phys.* **1997**, *56*, 3632−3635.
(40) Hass, J.; Feng, R.; Li, T.; Li, X.; Zong, Z.; de Heer, W. A.; First, P. N.; Conrad, E. H.; Jeffrey, C. A.; Berger, C. Highly ordered graphene for two dimensional electronics. *Appl. Phys. Lett.* **2006**, *89*, 143106.
(41) Dupuy, J. C.; Sibai, A.; Vilotitch, B. Mirror Electron-Microscopy (Mem) - Work Function and Imaging of an Electron-Beam Biased Junction of Silicon(100). *Surf. Sci.* **1984**, *147*, 191−202.
(42) Kennedy, S. M.; Zheng, C. X.; Tang, W. X.; Paganin, D. M.; Jesson, D. E. Caustic imaging of gallium droplets using mirror electron microscopy. *Ultramicroscopy* **2011**, *111*, 356−363.
(43) Shimakura, T.; Takahashi, Y.; Sugaya, M.; Ohnishi, T.; Hasegawa, M.; Ohta, H. Mirror electron microscope for inspecting nanometer-sized defects in magnetic media. *Microelectron. Eng.* **2008**, *85*, 1811−1814.
(44) Mavrikakis, M.; Hammer, B.; Norskov, J. K. Effect of strain on the reactivity of metal surfaces. *Phys. Rev. Lett.* **1998**, *81*, 2819−2822.
(45) Wintterlin, J.; Zambelli, T.; Trost, J.; Greeley, J.; Mavrikakis, M. Atomic-scale evidence for an enhanced catalytic reactivity of stretched surfaces. *Angew. Chem., Int. Ed.* **2003**, *42*, 2850−2853.
(46) Starodub, E.; Bartelt, N. C.; McCarty, K. F. Oxidation of Graphene on Metals. *J. Phys. Chem. C* **2010**, *114*, 5134−5140.
(47) Varykhalov, A.; Sanchez-Barriga, J.; Shikin, A. M.; Biswas, C.; Vescovo, E.; Rybkin, A.; Marchenko, D.; Rader, O. Electronic and Magnetic Properties of Quasifreestanding Graphene on Ni. *Phys. Rev. Lett.* **2008**, *101*, 157601.
(48) Varykhalov, A.; Gudat, W.; Rader, O. Imaging Buried Molecules: Fullerenes Under Graphene. *Adv. Mater.* **2010**, *22*, 3307−3310.
(49) Liao, Q.; Zhang, H. J.; Wu, K.; Li, H. Y.; Bao, S. N.; He, P. Oxidation of graphene on Ru(0001) studied by scanning tunneling microscopy. *Appl. Surf. Sci.* **2010**, *257*, 82−86.
(50) Riedl, C.; Coletti, C.; Iwasaki, T.; Zakharov, A. A.; Starke, U. Quasi-Free-Standing Epitaxial Graphene on SiC Obtained by Hydrogen Intercalation. *Phys. Rev. Lett.* **2009**, *103*, 246804.
(51) Oida, S.; McFeely, F. R.; Hannon, J. B.; Tromp, R. M.; Copel, M.; Chen, Z.; Sun, Y.; Farmer, D. B.; Yurkas, J. Decoupling graphene from SiC(0001) via oxidation. *Phys. Rev. B: Condens. Matter Mater. Phys.* **2010**, *82*, 041411.
(52) Watcharinyanon, S.; Virojanadara, C.; Osiecki, J. R.; Zakharov, A. A.; Yakimova, R.; Uhrberg, R. I. G.; Johansson, L. I. Hydrogen intercalation of graphene grown on 6H-SiC(0001). *Surf. Sci.* **2011**, *605*, 1662−1668.
(53) Goriachko, A.; Over, H. Modern Nanotemplates Based on Graphene and Single Layer h-BN. *Z. Phys. Chem.* **2009**, *223*, 157−168.
(54) Goriachko, A.; Zakharov, A. A.; Over, H. Oxygen-etching of h-BN/Ru(0001) nanomesh on the nano- and mesoscopic scale. *J. Phys. Chem. C* **2008**, *112*, 10423−10427.